2013

Response of green reflectance continuum removal index to the xanthophyll de-epoxidation cycle in Norway spruce needles

Daniel Kovac
Academy of Sciences of the Czech Republic, kovac.d@czechglobe.cz

Zbynek Malenovsky
University of Tasmania, zbynek@uow.edu.au

Otmar Urban
Academy of Sciences of the Czech Republic

Vladimir Spunda
Academy of Sciences of the Czech Republic

Jiri Kalina
University of Ostrava

See next page for additional authors

Publication Details

Kovac, D., Malenovsky, Z., Urban, O., Spunda, V., Kalina, J., Ac, A., Kaplan, V. & Hanus, J. (2013). Response of green reflectance continuum removal index to the xanthophyll de-epoxidation cycle in Norway spruce needles. Journal of Experimental Botany, 64 (7), 1817-1827.

Response of green reflectance continuum removal index to the xanthophyll de-epoxidation cycle in Norway spruce needles

Abstract

A dedicated field experiment was conducted to investigate the response of a green reflectance continuum removal-based optical index, called area under the curve normalized to maximal band depth between 511nm and 557nm (ANMB511-557), to light-induced transformations in xanthophyll cycle pigments of Norway spruce [Picea abies (L.) Karst] needles. The performance of ANMB511-557 was compared with the photochemical reflectance index (PRI) computed from the same leaf reflectance measurements. Needles of four crown whorls (fifth, eighth, 10th, and 15th counted from the top) were sampled from a 27-year-old spruce tree throughout a cloudy and a sunny day. Needle optical properties were measured together with the composition of the photosynthetic pigments to investigate their influence on both optical indices. Analyses of pigments showed that the needles of the examined whorls varied significantly in chlorophyll content and also in related pigment characteristics, such as the chlorophyll/carotenoid ratio. The investigation of the ANMB511-557 diurnal behaviour revealed that the index is able to follow the dynamic changes in the xanthophyll cycle independently of the actual content of foliar pigments. Nevertheless, ANMB511-557 lost the ability to predict the xanthophyll cycle behaviour during noon on the sunny day, when the needles were exposed to irradiance exceeding 1000 μmol m-2 s-1. Despite this, ANMB511-557 rendered a better performance for tracking xanthophyll cycle reactions than PRI. Although declining PRI values generally responded to excessive solar irradiance, they were not able to predict the actual de-epoxidation state in the needles examined.

Keywords

Chlorophyll to carotenoid ratio, continuum removal, excessive irradiance, leaf reflectance, spectral index, xanthophyll cycle pigments

Disciplines

Medicine and Health Sciences | Social and Behavioral Sciences

Publication Details

Kovac, D., Malenovsky, Z., Urban, O., Spunda, V., Kalina, J., Ac, A., Kaplan, V. & Hanus, J. (2013). Response of green reflectance continuum removal index to the xanthophyll de-epoxidation cycle in Norway spruce needles. Journal of Experimental Botany, 64 (7), 1817-1827.

Authors

Daniel Kovac, Zbynek Malenovsky, Otmar Urban, Vladimir Spunda, Jiri Kalina, Alexander Ac, Veroslav Kaplan, and Jan Hanus

Response of green reflectance continuum removal index to xanthophyll de-epoxidation cycle in Norway spruce needles

Daniel Kováč[A,E], *Zbyněk Malenovský*[B,D], *Otmar Urban*[A], *Vladimír Špunda*[A,C], *Jiří Kalina*[C], *Alexander Ač*[A]., *Věroslav Kaplan*[A], *Jan Hanuš*[A]

[A]Global Change Research Centre, Academy of Sciences of the Czech Republic, Bělidla 4a, CZ-603 00 Brno, Czech Republic
[B]School of Geography and Environmental Studies, University of Tasmania, Private Bag 76, Hobart 7001, Australia
[C]Department of Physics, Faculty of Science, University of Ostrava, Chittussiho 10, CZ-71000 Slezská Ostrava, Czech Republic
[D]Remote Sensing Laboratories, Department of Geography, University of Zürich, Winterthurerstrasse 190, CH-8057 Zürich, Switzerland
[E]Corresponding author. Email: kovac.d@czechglobe.cz

ABSTRACT

A dedicated field experiment was conducted to investigate the response of a green reflectance continuum removal-based optical index called Area under curve Normalized to Maximal Band depth between 511-557 nm ($ANMB_{511-557}$) to light-induced transformations in xanthophyll cycle pigments of Norway spruce *(Picea abies (L.)* Karst) needles. Performance of $ANMB_{511-557}$ was compared with the Photochemical Reflectance Index (PRI) computed from the same leaf reflectance measurements. Needles of four crown whorls (5^{th}, 8^{th}, 10^{th} and 15^{th} counted from the top) were sampled from a 27-year old spruce tree throughout a cloudy and sunny day. Needle optical properties were measured together with the composition of the photosynthetic pigments to investigate their influence on both optical indices. Analyses of pigments showed that the needles of the examined whorls varied significantly in chlorophyll content and also in related pigment characteristics, e.g. chlorophyll/carotenoids ratio. The investigation of the $ANMB_{511-557}$ diurnal behavior revealed that the index is able to follow the dynamic changes in the xanthophyll cycle independently of the actual content of foliar pigments. Nevertheless, $ANMB_{511-557}$ lost the xanthophyll cycle behavior predictability during noontime of the sunny

day, when the needles were exposed to irradiance exceeding 1000 μmol m^{-2} s^{-1}. Despite of this, $ANMB_{511-557}$ rendered a better performance for tracking xanthophyll cycle reactions than PRI. Although declining PRI values generally responded to excessive solar irradiance, they were not able to predict actual de-epoxidation state in examined needles.

KEYWORDS: continuum removal, chlorophylls to carotenoids ratio, excessive irradiance, leaf reflectance, spectral index, xanthophyll cycle pigments

INTRODUCTION

Thermal energy dissipation through the xanthophyll cycle is a photoprotective mechanism that was developed by plants to keep the delicate balance between efficient light harvesting under limited irradiance and regulated energy dissipation under excess irradiance (Adir *et al.*, 2003). The xanthophyll cycle involves the enzymatic de-epoxidation of violaxanthin (V) to zeaxanthin (Z) via antheraxanthin (A) and re-epoxidation of Z to V via A (Yamamoto, 1979; Demmig-Adams and Adams, 2006). Under high irradiations, a high proton gradient across the thylakoid lumen promotes the conversion of V into Z, whereas under low light intensities or darkness the low thylakoid proton gradient induces the epoxidation of Z into V. The photoprotective V-Z conversion lowers the energy level of the lowest excited singlet state below that of chlorophyll *a* (Chl *a*), providing a sink for the excess excitation energy (Frank *et al.*, 1994). Upon Z–Chl *a* enclosure, excess light energy is being released in the process called non-photochemical quenching of Chl *a* fluorescence in PSII (Krause and Weis, 1991). Z–Chl *a* enclosure is mediated through conformational changes in photosystem II (PSII) and co-adjacent light harvesting antennae complex (LHCII), which is also induced by thylakoid acidification.

The xanthophyll cycle engagement into photosynthesis regulation through excess light energy dissipation in PSII has been widely documented, for instance by Pfündel and Bilger (1994). Based on this finding, the Photochemical Reflectance Index (PRI) was proposed as a physiologically based optical index responding to changes in the xanthophyll cycle through fluctuations in 531 nm reflectance (Gamon *et al.*, 1992). Measurements of individual leaves have demonstrated a significant PRI relationship to the effective PSII quantum yield (ΦPSII), a fluorescence based indicator of PSII light use efficiency (LUE), and also to LUE calculated from gas exchange measurements in leaves of several species (Peñuelas *et al.*, 1995). A strong PRI reduction was observed simultaneously with severe LUE reduction during midday in long-living and slow-growing evergreens having a higher maximal capacity for flexible thermal dissipation due to a higher VAZ pigment possession (Peñuelas *et al.*, 1995; Peguero-Pina *et al.*, 2008). On the other hand, several studies applying PRI at canopy level showed that the relationship between photosynthetic efficiency and PRI is inconsistent over time, likely due to the changes in foliar pigment content and canopy architecture changing ratio between sunlit and shaded leaves (Barton and North, 2001; Filella *et al.*, 2004). It has been shown that the degradation of foliar chlorophylls generally reduces PRI as a result of the relative reflectance increase at 570 nm (Moran *et al.*, 2000; Nakaji *et al.*, 2006; Sims and Gamon, 2002). This PRI dependency on foliage chlorophyll content and on the chlorophyll/carotenoids ratio (Chl *a*+*b*/ Car *x*+*c*) was eventually used to track seasonal alterations in photosynthetic activity (Filella *et al.*, 2009; Stylinski *et al.*, 2002).

We tested a potential use of continuum-removed reflectance of green wavelengths for tracking the xanthophyll cycle dynamic in our previous laboratory experiments with Norway spruce seedlings (Kováč *et al.*, 2012). The spectral index named Area under curve Normalized to Maximal Band depth (ANMB) (Malenovský *et al.*, 2006b) was calculated from leaf reflectance spectra between 510–555 nm (borders of wavelength interval ± 3 nm). ANMB was found to follow alterations in the leaf xanthophyll de-epoxidation state (DEPS), while staying insensitive to the actual content of foliar pigments (i.e. total chlorophylls, Chl *a*+*b*/ Car *x*+*c* ratio and VAZ pool size). These results were obtained from the analysis of more than 200 spruce needle reflectance measurements recorded after the acclimation of spruce seedlings to controlled pre-defined microclimatic conditions inside the laboratory growth chambers.

The main objective of this study is, therefore, to explore the behavior of the ANMB index in the case of mature Norway spruce (*Picea abies [L.]* Karst.) trees that are exposed to complex outdoor environmental conditions and forced to adapt fast to different diurnal irradiation regimes. The field experiment focuses on investigating the relationship between the xanthophyll cycle dynamic and both ANMB and PRI under uncontrolled varying natural illumination conditions of a cloudy and a sunny day.

MATERIAL AND METHODS

Plant material and experimental design

The experiment was conducted in the forest stand located at the Experimental ecological site Bílý Kříž (Beskydy Mountains, 49°33´N, 18°32´E, NE of the Czech Republic, 908 m a.s.l.). The experimental forest stand of 6.2 ha was planted in 1981 with 4-year old seedlings of *Picea abies (L.)* Karst. on a slope ranging from 11° to 16° with SSW exposition. The stand density was, at the time of the experiment, about 1430 trees.ha^{-1}, with the hemi-surface leaf area index (LAI) equal to 9.5 m^2 m^{-2} with a standard deviation (STD) of ± 0.27 m^2 m^{-2}. The mean tree height was 13.4 m (STD = ± 0.1 m).

The measurements were performed on two days in July 2008 with different sky conditions, i.e. a prevailingly cloudy and a sunny day (Fig. 1). During the first measurement day the diffuse-to-total irradiation ratio (DI; diffuse index) was mostly above 0.7, whereas during the sunny periods of the second day it was less than 0.3 (Fig. 1B). The average microclimatic conditions during the three days preceding the measurements were similar to those on the measurement day (data not shown). Additionally, rather heavy rain was falling for those three days prior to the measurements on the cloudy day (total three-day precipitation of 73 mm), whereas it was not raining for four days prior to the measurements on the sunny day.

Needles of different types and age classes with S/SW orientation were selected for the measurements: from the 5th whorl (counted from the apex top of the tree): 1-year old shoots, from the 8th and 10th whorl: 2-year old shoots, and from the 15th whorl: shoots older than 2 years. The measurement of the needle samples was performed four times throughout the day, i.e. approximately at dawn – D (c. 5.00 GTM+1), morning – M (c. 8.00 GTM+1), noon – N (c. 13.00 GTM+1), and afternoon – A (c. 18.00 GTM+1). Needle samples removed from the tree were partially measured for their optical properties and partially stored in liquid nitrogen for the laboratory pigment analysis. In an effort to capture the investigated daily dynamics as accurately as possible, the needle optical properties were measured immediately after removing the shoots from the tree. Arranging the needles in the carrier for the optical property measurements took approximately 5 minutes. All measurements were completed within 10 minutes after removing the needles from the shoot. Our previous laboratory tests showed no significant change in DEPS of spruce needles within 10 minutes after their detachment from the shoot (unpublished data). Therefore, the processing time is considered to be short enough to prevent any significant change in the leaf xanthophyll composition. Needles collected for the pigment analysis were weighted and their projected area was acquired using a digital table scanner. To readapt to the irradiation conditions before their collection, for following 10 minutes they were exposed to irradiation of the same intensity as recorded during the *in-situ* measurement with LI-190 (Li-Cor, Lincoln, NE, USA) quantum sensor (Fig. 1CD). Light-adapted needles were stored frozen in liquid nitrogen until they were processed for pigment analysis in the laboratory.

Reflectance measurements

Since coniferous leaves are small and narrow objects, Daughtry's method described in Mesarch et al. (1999) and adjusted for narrow and short Norway spruce needles by Malenovský et al. (2006a) was applied to measure the leaf optical properties. The determination of spruce needle reflectance was based on the comparison of the total sample reflectance flux (R_{TOTAL}) against the reflectance of a $BaSO_4$ reference panel (R_{REF}), both measured separately inside an integrating sphere LI-1800-12 (Li-Cor, USA) coupled with a field spectroradiometer ASD FieldSpec-3 (ASD Inc., Colorado, USA). The spruce needle directional-hemispherical reflectance (R) between 400–1100 nm, with a wavelength interval of 1 nm, was calculated according to the equation:

$$R = \frac{R_{TOTAL} / R_{REF}}{1 - GF}, \quad \text{(Eq. 1)}$$

where GF is the gap fraction, i.e. the fraction of the air gaps between the needles of the sample measured in reflectance mode. To obtain the GF of illuminated needles, the sample holder with needles inside was placed in a conventional double lamp table scanner and an image of area illuminated during the reflectance measurement was acquired. The determination of the GF was done by dividing the number of pixels of all the gaps between the needles by the number of pixels of the illuminated (measured) area in an image processing software. The scanned needles were not used for any further analysis. The GF values of the measured samples ranged from 0.2 to

0.3. Finally, the PRI was calculated from the leaf reflectance (R_λ) of two wavelengths (λ ~ 531 and 570 nm) as PRI = $(R_{531}-R_{570})/(R_{531}+R_{570})$.

Optical index $ANMB_{511-557}$

The Area under curve Normalized to Maximal Band depth between 511-557 nm ($ANMB_{511-557}$) is an optical index based on a the mathematical transformation of reflectance absorption features called continuum removal (Broge and Leblanc, 2001; Kokaly and Clark, 1999). The detailed description of ANMB index design can be found in Malenovský et al. (2006b) and recently also in Kováč et al. (2012). The $ANMB_{511-557}$ calculation consists of two consecutive steps. In the first, the Area Under Curve of continuum-removed reflectance between 511 and 557 nm ($AUC_{511-557}$) is calculated according to the equation:

$$AUC_{511-557} = \frac{1}{2}\sum_{i=1}^{n-1}(\lambda_{i+1} - \lambda_i)(R_{CR(\lambda i+1)} + R_{CR(\lambda i)}), \qquad \text{(Eq. 2)}$$

where $R_{CR(\lambda i)}$ and $R_{CR(\lambda i+1)}$ are the continuum-removed reflectance values of the spectral bands at the wavelengths λ_i and λ_{i+1} located within the spectral interval 511 – 557 nm (spectral resolution of 1 nm), and n is the number of spectral bands, which is, in this case, equal to 47,

In the second, the $ANMB_{511-557}$ index is computed as the ratio of $AUC_{511-557}$ and a maximal band depth of the continuum-removed reflectance between 511-557 nm ($MBD_{511-557}$):

$$ANMB_{511-557} = \frac{AUC_{511-557}}{MBD_{511-557}}. \qquad \text{(Eq. 3)}$$

The reflectance of the selected wavebands is influenced by the xanthophyll cycle pigments conversion, which was first detected and reported as leaf reflectance fluctuation at 526 nm by Gamon et al. (1997). Making use of several bands of the green spectral region combined within the $ANMB_{511-557}$ index was found to be yet another efficient way how to retrieve information on the rate of xanthophyll de-epoxidation (Kováč *et al.*, 2012).

Foliar pigment analysis

The light adapted needle samples, transported frozen in liquid nitrogen to the laboratory, were homogenized in 80% acetone with a small amount of $MgCO_3$, and centrifuged (480 rpm) at room temperature for 3 min. The contents of chlorophyll *a* (Chl *a*), chlorophyll *b* (Chl *b*) and total carotenoids (Car *x+c*) in the supernatant were determined spectrophotometrically (UV/VIS 550, Unicam, Cambridge, UK) from absorbances measured at 470, 646.8, 663.2, and 750 nm according to the equations presented by Lichtenthaler (1987). Chl *a+b* and Car *x+c* contents were expressed per unit needle area that was estimated via scanned digital images of samples analyzed by the Cernota software (Kalina and Slovák, 2004). The relative amounts of the xanthophyll cycle pigments, i.e. antheraxanthin (A), violaxanthin (V), and zeaxanthin (Z), were obtained from HPLC pigment analyses (Kurasová *et al.*, 2003). The conversion factors for contents of the individual carotenoids (i.e. the pool of the xanthophyll cycle pigments; VAZ) and chlorophylls were applied according to Färber and Jahns (1998). The conversion state of the xanthophyll cycle pigments (i.e. de-epoxidation state; DEPS) was calculated according to Gilmore and Björkman (1994) as:

$$DEPS = [A + Z]/ [V + A + Z]. \qquad \text{(Eq. 4)}$$

Statistical data analysis

Statistically significant differences of means were tested using a two-sample F-test for variances, followed by a Student's t-test with the level of significance $P < 0.05$. Based on the results of the F-test, a t-test, assuming either equal or unequal variances, was applied.

The determination coefficient (R^2) was computed to express the variation percentage of a dependent variable explained by an established regression to the independent variable. The significance of the statistical model was tested at probability levels $P < 0.05$, $P < 0.01$, and $P < 0.001$, using the analysis of variance (ANOVA).

All calculations and tests were conducted in the R mathematical-statistical programming environment (R Development Core Team2010).

RESULTS AND DISCUSSION

Composition of photosynthetic pigments in needle samples during sunny and cloudy days

Plant material collected from each level of the spruce crown differed in the morphometric parameter specific leaf area (SLA). On both experimental days, the highest SLA values were observed for needles of the 10^{th} whorl, and the lowest for needles of the 5^{th} and the 8^{th} whorls (Fig. 2A, $P < 0.05$).

The total chlorophyll content (Chl *a+b*) in needles collected from each crown level during the sunny and cloudy day varied within the range shown in figure 2B. Chl *a+b* of the 5^{th} and 8^{th} whorl sampled on the sunny day was in average about 0.05 g m^{-2} higher than Chl *a+b* examined on the cloudy day ($P < 0.05$). This difference increased the Chl *a+b*/Car *x+c* ratio in needles of the 5^{th} whorl on the sunny day (Fig. 2D, $P < 0.05$), whereas the Chl *a+b*/Car *x+c* ratio in needles of the 8^{th} whorl remained within the original range of the cloudy day. Similarly, needles from mostly shaded lower levels of the crown (10^{th} and 15^{th} whorl) did not exhibit significant Chl *a+b*/Car *x+c* differences between both experimental days (Fig. 2D). Their Chl *a+b*/Car *x+c* ratios are consistent with the previous finding of (Sarijeva *et al.*, 2007) suggesting that Chl *a+b*/Car *x+c* ratio of shaded leaves is higher due to the higher LHCII possession.

The pool size of the xanthophyll cycle pigments (VAZ) follows clearly the sun-to-shade crown gradient, being larger in sunlit and smaller in shaded leaves (Fig. 2C, $P < 0.05$). The statistically significant difference highlights the importance of the xanthophyll cycle for photoprotection in each particular needle type (Demmig-Adams, 1998). In sunlit needles, VAZ/Chl *a+b* is similar for needles sampled on the sunny day despite the increase in Chl *a+b*. Although, not being statistically different, the VAZ pool in needles of the 5^{th} whorl increased slightly on the sunny day compared to the pool on the cloudy day.

Dynamic conversions of the xanthophyll cycle pigments during the cloudy and sunny day

At dawn (D) of both days the needle DEPS of all whorls was nearly the same, i.e. around 15% (Fig. 3). As expected and observed previously (Demmig-Adams *et al.*, 1999), zeaxanthin reached the maximal conversional state during noon of both sky conditions. The highest conversional rate of xanthophyll cycle pigments was found on the sunny day in sunlit needles of the 5th and 8th whorl (Fig. 3B). In this part of the crown, DEPS in the morning (M) of the sunny day reached values around 60-70%. DEPS between 70-75% was peaking at noon (N) under the irradiance of about 1000 μmol.m^{-2}.s^{-1}. In the late afternoon (A), the DEPS dropped down to 25% and 45% in needles of the 5th and 8th whorl, respectively.

A relatively low noon DEPS of 39.3% in needles of the 5th whorl after a relatively clear sky window between 9:30 am and 11:30 am of the cloudy day (Fig. 1A) is comparable with morning DEPS of 34.1% (Fig. 3A). The DEPS did not increase significantly or quickly relaxed close to the morning state. Either way, it did not persist at a high level as usually observed after a high solar illumination in conditions of an additional stress, e.g. intensive drought (Baraldi *et al.*, 2008). This suggests that during our experiment the examined tree was not stressed by any other environmental factor but high irradiance. At noon of the cloudy day the DEPS of 56% in needles of the 8th whorl (Fig. 3A) was accompanied by a low possession of VAZ pigments. In this particular case, the Chl *a+b* of 8th whorl needles was 2% lower compared to that in 5th whorl needles, and the VAZ/Chl *a+b* ratio of 5th whorl needles was 12% higher ($P < 0.05$) than that in needles of the 8th whorl. Finally, for both days the DEPS diurnal patterns of 10th and 15th whorl needles were similar to that observed in sunlit needles of the 5th and 8th whorl, but with a lower VAZ conversional state (Fig. 3).

Photochemical Reflectance Index (PRI)

Mean reflectance spectra collected for needles of all four whorls investigated during both experimental days are shown in Fig. 4. Standard error bars indicate the reflectance variability at wavelengths of 550 nm and 800 nm. Shape and amplitude of the needle reflectance signatures indicate systematic changes in foliar pigments and also in geometrical and structural needle characteristics as previously observed by Malenovský et al. (2006b). Even though pigment analyses were not performed on plant material used for optical measurements, the causal correspondence that can be observed between the visible and near infrared reflectance in Fig. 4 and pigment content and SLA measurements in Fig. 2 displays a good representation of spectral signatures for each crown level.

Diurnal courses of the PRI index computed from needle directional-hemispherical reflectance of four investigated whorls acquired during the cloudy and sunny day are shown in Fig. 5. PRI values are positive in most cases, which is in accordance with the results reviewed in Garbulsky et al. (2011). Negative PRI values were typically reported for leaves under strong light stress, which induces photoprotective reactions resulting in low light use efficiency. In our experiment these would be needles of the 5th and 8th whorl in late morning, noon, and afternoon on the sunny day. PRI was, however, reaching negative values only for needles of the 8th whorl at noon, for the remaining needle samples it was close to zero, but positive. Also, expected daily changes in PRI due to the increasing solar irradiation are not obvious (Fig. 5). This can be explained by the fact that PRI values are not functionally dependent only on xanthophyll de-epoxidation, but also on the actual pool of carotenoids and chlorophylls (Sims and Gamon, 2002). Results in Fig. 6 show that our PRI values are in general lower for foliage experiencing a stronger light with the photosynthetic photon flux density (PPFD) reaching or exceeding 1000 µmol m^{-2} s^{-1} (i.e. 5th and 8th whorl on the sunny day) and having a lower Chl $a+b$/ Car $x+c$ ratio (Cheng *et al.*, 2012). Higher PRI values can indicate either medium DEPS combined with a lower Chl $a+b$/ Car $x+c$ ratio or low DEPS combined with a higher Chl $a+b$/ Car $x+c$ ratio (compare Fig. 3 and Fig. 6). Consequently, the interpretation of the PRI values measured under PPFD below 300 µmol m^{-2} s^{-1} (i.e. all whorls on the cloudy day and the 10th and 15th whorl on the sunny day; Fig. 1.) is ambiguous due to the differences in pigment content. This ambiguity may also explain an insignificant regression relation that we observed between the PRI and DEPS measurements (results not shown).

$ANMB_{511\text{-}557}$ index

$ANMB_{511\text{-}557}$ was designed as the ratio of the area under continuum-removed reflectance between 511-557 nm ($AUC_{511\text{-}557}$) and the depth of this feature ($MBD_{511\text{-}557}$) (Eq. 3). Although $AUC_{511\text{-}557}$ carries valuable information about reflectance losses caused by xanthophyll de-epoxidation, it is also influenced by the fluctuation of green reflectance due to the varying chlorophyll pigments composition and mass (Fig. 4). Consequently $AUC_{511\text{-}557}$ and also $MBD_{511\text{-}557}$ do not exhibit a strong dependency on DEPS (Fig. 7), but being shaped by similar driving forces their ratio is able to eliminate the undesirable chlorophyll influence and to emphasize a tiny xanthophyll de-epoxidation signal carried by $AUC_{511-557}$. Fig. 8 shows clearly the systematic difference between $AUC_{511-557}$ normalized by $MBD_{511-557}$ for DEPS equal to 13.5, 34.1 and 71.6%. Main advantage of the ANMB method is in avoidance of the reflectance at 570 nm, which has been identified as the cause of PRI instability by Moran et al. (2000) and later by Nakaji et al. (2006). As illustrated in Fig. 6, the PRI values are dependent on changes in leaf Chl $a+b$ and Car $x+c$ pigment pools, which are responsible for variations in leaf reflectance at 570 nm.

Diurnal changes of the $ANMB_{511-557}$ index during both experimental days are displayed in Fig. 9. Graphs are showing that the $ANMB_{511-557}$ values of the 5^{th}, 8^{th}, and 10^{th} whorl needles follow the alterations in xanthophyll's DEPS (Fig. 3) during the cloudy day as well as in the case of the 10^{th} whorl needles sampled on the sunny day. Needles of the 15^{th} whorl, however, do not show the diurnal pattern of $ANMB_{511-557}$ following temporal changes in DEPS, which might be caused by their low content of xanthophyll cycle pigments (VAZ) in general (see Fig. 2C). Similarly, no relation to DEPS was found for the needles of the 5^{th} and 8^{th} whorl on the sunny day due to the strong outlying deviation in $ANMB_{511-557}$ diurnal behaviour observed at noontime.

These results confirm, in general, our previous findings showing the ability of the ANMB index to assess the dynamics of the xantophyll cycle in needles of spruce seedlings kept under controlled and systematically varied environmental conditions (Kováč *et al.*, 2012). Contrary to this laboratory study, the $ANMB_{511-557}$ field measurements are deviating from the expected diurnal course in the case of sunlit needles (the 5^{th} and 8^{th} whorl) during noontime of the sunny day. Although PPFD of both experiments reached up to 1000 µmol m^{-2} s^{-1} (Fig. 1D), the field ANMB values suddenly increased due to the unexpected drop in $MBD_{511-557}$. At this stage, we have no indication explaining this mismatching ANMB behavior. Based on the findings of previous studies we assume that other physiological processes regulating the plant's photosynthetic capacity, e.g. non-assimilatory electron transport (Munekaga *et al.*, 2004) or photorespiration (Kangasjarvi *et al.*, 2012), may interfere with indicative ability of $ANMB_{511-557}$. The fact that the cause is at this point unknown suggests that follow-up experiments focusing on plant physiological differences between both experiments are needed to investigate this phenomenon.

Significance of the $ANMB_{511\text{-}557}$ relationship to xanthophyll changes

Despite the fact that most of the needle $ANMB_{511\text{-}557}$ and DEPS measurements do share similar diurnal patterns, a linear regression between $ANMB_{511\text{-}557}$ and DEPS of the 5^{th}, 8^{th}, and 10^{th} whorl needles was found to be insignificant. Statistically significant negative regressions were found only for values of the first two whorls corresponding to DEPS between 13% and 72% (i.e. between low and moderate PPFDs, measurements acquired at noon of the sunny day were excluded), the coefficient of the determination $R^2 = 0.61$ ($P < 0.001$), and of the 10^{th} whorl, the coefficient of the determination equal to 0.63 ($P < 0.05$). The fact that these significant dependencies were found in needles with a considerable variability in Chl *a+b* and Chl *a+b*/ Car *x+c* (Fig. 2) suggests that $ANMB_{511\text{-}557}$ is independent of the apparent content of foliar pigments. On the other hand, we noticed that an increase in $ANMB_{511\text{-}557}$ of needles from the 8^{th} whorl on the cloudy day corresponds with the increase in sample SLA (compare Fig. 2A with Fig. 8). An explanation of this correlation can be found in reflectance measurements, which were corrected for the air gap fraction between measured needles. This correction is less accurate in the case of small sized and strongly arched spruce needles (i.e. low SLA). Therefore, statistically higher SLA for the needles from the 10^{th} whorl compared to the needles of the 8^{th} and 5^{th} whorl might be the reason why our $ANMB_{511\text{-}557}$ values originating from different crown levels are incomparable, even though they correspond with similar DEPS. The influence of SLA on leaf $ANMB_{511\text{-}557}$ of broadleaf plants and coniferous species with long bifacial needles (e.g. pines) is expected to be negligible. Finally, we acknowledge that the extension of our sampling scheme, that would ensure full representation of the canopy heterogeneity, might help us to clarify the inconsistencies found between the optical indices and DEPS.

Perspective of the introduced $ANMB_{511\text{-}557}$ index

Our experiment suggests that PRI may not be the most efficient diurnal indicator of xanthophyll cycle photoprotection. The variations of Chl *a+b*/ Car *x+c* in needles measured are discussed as possible cause of low PRI performance in tracking DEPS of each crown level examined. A number of studies also pointed out that canopy PRI is dependent upon sensor viewing geometry (Hilker *et al.*, 2008; Middleton *et al.*, 2009). PRI values are higher when more shaded foliage with higher Chl *a+b*/ Car *x+c* and less soil contamination is being observed (Cheng *et al.*, 2010). Taking into account only sunlit leaves leads to an underestimation of canopy PRI, relatively to the actual photosynthesis performance (Goerner *et al.*, 2011). Realizing that combining information from strongly photosynthetically down-regulated sunlit and less down-regulated shaded foliage is essential for correct canopy PRI interpretation, Hilker *et al.* (2010) investigated PRI dependency on sensor viewing geometry and proposed a multiangular observation algorithm estimating the light use efficiency across different biomes. Although Malenovský et al. (2013) recently demonstrated independency of a continuum removal based optical index on canopy leaf area index, the newly proposed $ANMB_{511\text{-}557}$ index computed for vegetation canopies observed under different sensor viewing angles will need a similar treatment. Nevertheless, being insensitive to the changes in Chl *a+b* and Car *x+c* pigments' composition, the $ANMB_{511\text{-}557}$ index is expected to provide more accurate estimation of the actual stress response to solar irradiation at the canopy scale. The first step in this direction is improvement of the index performance for irradiances with PPFD exceeding 1000 μmol m^{-2} s^{-1}. The second step should take $ANMB_{511\text{-}557}$ through a multi-criterion sensitivity analysis investigating its applicability for canopies of different structural complexity and for airborne and space borne observations of different spectral, spatial and temporal specifications.

CONCLUSIONS

In this study we investigated in the field, i.e. under natural environmental conditions, the performance of a new spectroscopy indicator for a rapid assessment of the xanthophyll cycle state of plant leaves. Our results demonstrate the possibility to track the xanthophyll de-epoxidation reactions in Norway spruce needles using the leaf reflectance continuum removal optical index termed Area under curve Normalized to Maximal Band depth between 511-557 nm ($ANMB_{511\text{-}557}$). Among all examined leaf characteristics, differences in the chlorophyll content and the Chl *a+b*/Car *x+c* ratio varied most significantly when comparing sun and shade adapted needles. None of them was, however, found to disturb the indicative ability of $ANMB_{511\text{-}557}$. The analysis of the $ANMB_{511\text{-}557}$ dependence on DEPS proved that the index can follow the photoprotective xanthophyll changes in plant leaves during the cloudy day. $ANMB_{511-557}$ was, nevertheless, unable to capture the decreasing DEPS trend that occurred at noon of the sunny day, i.e. under the actual irradiation above 1000 μmol m^{-2} s^{-1}. This $ANMB_{511-557}$ deviation has not been explained, but it is expected to be associated with an enhanced need for plant intensive photoprotection. The observed spectral deviation in $ANMB_{511-557}$ diurnal behaviour may affect the current concept of deriving light use efficiency (LUE) from reflectance data in general (Garbulsky *et al.*, 2011), and should therefore be further investigated. Also, the improvement of $ANMB_{511-557}$ performance and its potential use for estimating leaf or even canopy LUE remain objective of follow up studies.

ACKNOWLEDGEMENTS

This work is a part of the research supported by the grant projects ForChange (SP/2D1/70/08) and CzechTerra (SP/2d1/93/07) of the Ministry of Environment of the Czech Republic. It was also supported by the European Commission within the CzechGlobe project (contract CZ.1.05/1.1.00/02.0073) and by the Research Intention AV0Z60870520. We thank Mrs Běla Piskořová and Mr Ladislav Šigut of the Department of Physics at the University of Ostrava for analyzing the content of the photosynthetic pigments as well as Mrs Gabrielle Johnson for English language editing.

REFERENCES

Adir N, Zer H, Shochat S, Ohad I. 2003. Photoinhibition - a historical perspective. *Photosynthesis Research* **76**, 343-370.

Baraldi R, Canaccini F, Cortes S, Magnani F, Rapparini F, Zamboni A, Raddi S. 2008. Role of xanthophyll cycle-mediated photoprotection in Arbutus unedo plants exposed to water stress during the Mediterranean summer. *Photosynthetica* **46**, 378-386.

Barton CVM, North PRJ. 2001. Remote sensing of canopy light use efficiency using the photochemical reflectance index - Model and sensitivity analysis. *Remote Sensing of Environment* **78**, 264-273.

Broge NH, Leblanc E. 2001. Comparing prediction power and stability of broadband and hyperspectral vegetation indices for estimation of green leaf area index and canopy chlorophyll density. *Remote Sensing of Environment* **76**, 156-172.

Cheng YB, Middleton E, Zhang Q, Corp L, Dandois J, Kustas WP. 2012. The photochemical reflectance index from directional cornfield reflectances: Observations and simulations. *Remote Sensing of Environment* **124**, 444-453.

Demmig-Adams B. 1998. Survey of thermal energy dissipation and pigment composition in sun and shade leaves. *Plant and Cell Physiology* **39**, 474-482.

Demmig-Adams B, Adams WW, Ebbert V, Logan BA. 1999. Ecophysiology of the xanthophyll cycle. *Photochemistry of Carotenoids*, Vol. 8. Dordrecht: Kluwer Academic Publ, 245-269.
Demmig-Adams B, Adams WW. 2006. Photoprotection in an ecological context: the remarkable complexity of thermal energy dissipation. *New Phytologist* **172**, 11-21.
Färber A, Jahns P. 1998. The xanthophyll cycle of higher plants: influence of antenna size and membrane organization. *Biochimica Et Biophysica Acta-Bioenergetics* **1363**, 47-58.
Filella I, Peñuelas J, Llorens L, Estiarte M. 2004. Reflectance assessment of seasonal and annual changes in biomass and CO2 uptake of a Mediterranean shrubland submitted to experimental warming and drought. *Remote Sensing of Environment* **90**, 308-318.
Filella I, Porcar-Castell A, Munne-Bosch S, Back J, Garbulsky MF, Peñuelas J. 2009. PRI assessment of long-term changes in carotenoids/chlorophyll ratio and short-term changes in de-epoxidation state of the xanthophyll cycle. *International Journal of Remote Sensing* **30**, 4443-4455.
Frank HA, Cua A, Chynwat V, Young A, Gosztola D, Wasielewski MR. 1994. Photophysics of the carotenoids associated with the xanthophyll cycle in photosynthesis. *Photosynthesis Research* **41**, 389-395.
Gamon JA, Peñuelas J, Field CB. 1992. A NarrowWaveband Spectral Index That Tracks Diurnal Changes in Photosynthetic Efficiency. *Remote Sensing of Environment* **41**, 35-44.
Gamon JA, Serrano L, Surfus JS. 1997. The photochemical reflectance index: an optical indicator of photosynthetic radiation use efficiency across species, functional types, and nutrient levels. *Oecologia* **112**, 492-501.
Garbulsky MF, Peñuelas J, Gamon J, Inoue Y, Filella I. 2011. The photochemical reflectance index (PRI) and the remote sensing of leaf, canopy and ecosystem radiation use efficiencies A review and meta-analysis. *Remote Sensing of Environment* **115**, 281-297.
Gilmore AM, Björkman O. 1994. Adenine nucleotides and the xanthophyll cycle in leaves. II. Comparison of the effects of CO2- and temperature-limited photosynthesis on photosystem II fluorescence quenching, the adenylate energy charge and violaxanthin de- epoxidation in cotton. *Planta* **192**, 537-544.
Kalina J, Slovák V. 2004. The inexpensive tool for the determination of projected leaf area. *Ekologia-Bratislava* **23**, 163-167.
Kangasjarvi S, Neukermans J, Li SC, Aro EM, Noctor G. 2012. Photosynthesis, photorespiration, and light signalling in defence responses. *Journal of Experimental Botany* **63**, 1619-1636.
Kokaly RF, Clark RN. 1999. Spectroscopic determination of leaf biochemistry using band-depth analysis of absorption features and stepwise multiple linear regression. *Remote Sensing of Environment* **67**, 267-287.
Kováč D, Navrátil M, Malenovský Z, Štroch M, Špunda V, Urban O. 2012. Reflectance continuum removal spectral index tracking the xanthophyll cycle photoprotective reactions in Norway spruce needles. *Functional Plant Biology* **39**, 987-998.
Krause GH, Weis E. 1991. Chlorophyll fluorescence and photosynthesis: the basics *Annual Review of Plant Physiology and Plant Molecular Biology* **42**, 313-349.
Kurasová I, Kalina J, Urban O, Štroch M, Špunda V. 2003. Acclimation of two distinct plant species, spring barley and Norway spruce, to combined effect of

various irradiance and CO2 concentration during cultivation in controlled environment. *Photosynthetica* **41**, 513-523.
Lichtenthaler HK. 1987. Chlorophylls and carotenoids: Pigments of photosynthetic biomembranes. *Methods in Enzymology* **148**, 350-382.
Malenovský Z, Albrechtová J, Lhotáková Z, Zurita-Milla R, Clevers J, Schaepman ME, Cudlín P. 2006a. Applicability of the PROSPECT model for Norway spruce needles. *International Journal of Remote Sensing* **27**, 5315-5340.
Malenovský Z, Homolová L, Zurita-Milla R, Lukeš P, Kaplan V, Hanuš J, Gastellu-Etchegorry J-P, Schaepman, ME. 2013. Retrieval of spruce leaf chlorophyll content from airborne image data using continuum removal and radiative transfer. *Remote Sensing of Environment* **131**, 85-102.
Malenovský Z, Ufer CM, Lhotáková Z, Clevers JGPW, Schaepman ME, Albrechtová J, Cudlín P. 2006b. A new hyperspectral index for chlorophyll estimation of a forest canopy: Area under curve Normalized to Maximal Band depth between 650-725 nm. *EARSeL eProceedings* **5**, 161-172.
Mesarch MA, Walter-Shea EA, Asner GP, Middleton EM, Chan SS. 1999. A revised measurement methodology for conifer needles spectral optical properties: Evaluating the influence of gaps between elements. *Remote Sensing of Environment* **68**, 177-192.
Moran JA, Mitchell AK, Goodmanson G, Stockburger KA. 2000. Differentiation among effects of nitrogen fertilization treatments on conifer seedlings by foliar reflectance: a comparison of methods. *Tree Physiology* **20**, 1113-1120.
Munekaga Y, Hashimoto M, Miyaka C, Tomizawa KI, Endo T, Tasaka M, Shikanai T. 2004. Cyclic electron flow around photosystem I is essential for photosynthesis. *Nature* **429**, 579-582.
Nakaji T, Oguma H, Fujinuma Y. 2006. Seasonal changes in the relationship between photochemical reflectance index and photosynthetic light use efficiency of Japanese larch needles. *International Journal of Remote Sensing* **27**, 493-509.
Peguero-Pina JJ, Morales F, Flexas J, Gil-Pelegrin E, Moya I. 2008. Photochemistry, remotely sensed physiological reflectance index and de-epoxidation state of the xanthophyll cycle in Quercus coccifera under intense drought. *Oecologia* **156**, 1-11.
Peñuelas J, Filella I, Gamon JA. 1995. Assessment of photosynthetic radiation-use efficiency with spectral reflectance. *New Phytologist* **131**, 291-296.
Pfündel E, Bilger W. 1994. Regulation and possible function of the violaxanthin cycle. *Photosynthesis Research* **42**, 89-109.
R Development Core Team. 2010. R: A Language and Environment for Statistical Computing. R Foundation for Statistical Computing. Vienna, Austria., ISBN 3-900051-07-0.
Sarijeva G, Knapp M, Lichtenthater HK. 2007. Differences in photosynthetic activity, chlorophyll and carotenoid levels, and in chlorophyll fluorescence parameters in green sun and shade leaves of Ginkgo and Fagus. *Journal of Plant Physiology* **164**, 950-955.
Sims DA, Gamon JA. 2002. Relationships between leaf pigment content and spectral reflectance across a wide range of species, leaf structures and developmental stages. *Remote Sensing of Environment* **81**, 337-354.
Stylinski CD, Gamon JA, Oechel WC. 2002. Seasonal patterns of reflectance indices, carotenoid pigments and photosynthesis of evergreen chaparral species. *Oecologia* **131**, 366-374.

Yamamoto HY. 1979. Biochemistry of the violaxanthin cycle in higher plants. *Pure and Applied Chemistry* **51**, 639-648.

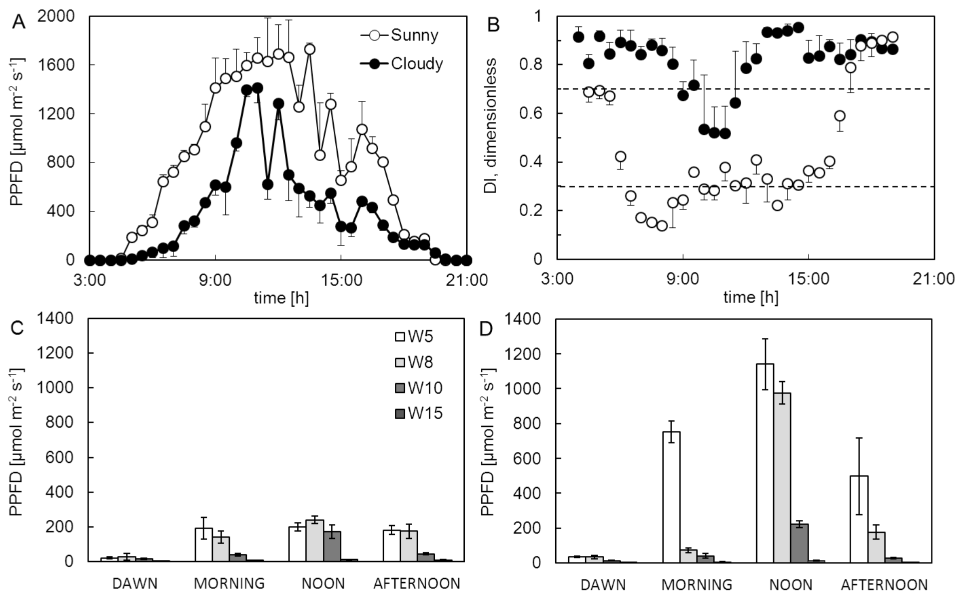

Fig. 1 Diurnal course of (A) photosynthetic photon flux density (PPFD) during investigated cloudy and sunny days as recorded by the quantum sensor LI-190SA (Li-Cor, USA) placed above the canopy, and (B) diffuse index (DI). The mean (dots) and standard deviations (error bars) of 30-min intervals are presented. Light environment at the level of the 5th (W5), 8th (W8), 10th (W10) and 15th (W15) whorl during the time of measurement on the (C) cloudy day and (D) sunny day as recorded by the LI-190SA sensor. Presented as mean and standard deviations of three measurements performed.

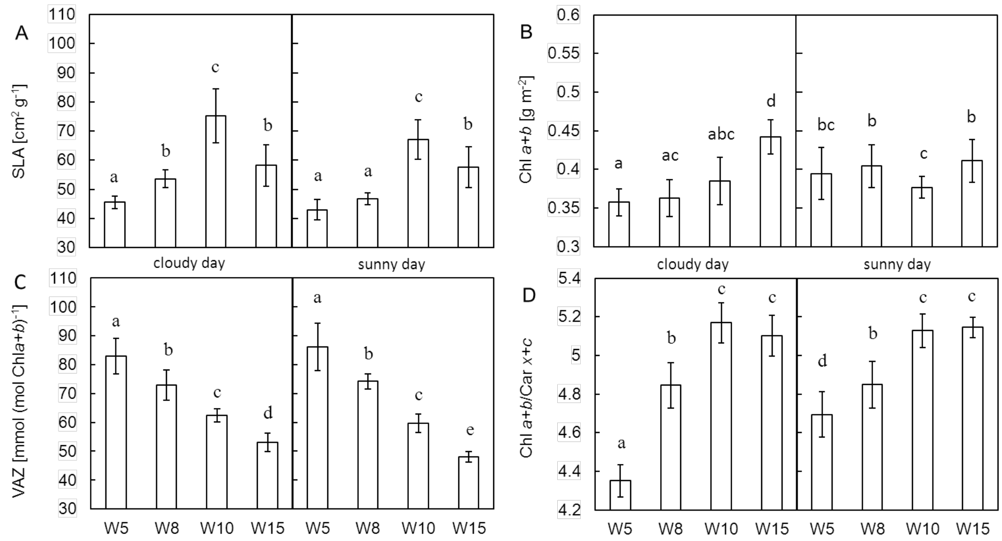

Fig. 2 Difference in (A) specific leaf area (SLA), (B) amount of chlorophyll *a*+*b* per unit leaf area, (C) content of xanthophyll cycle pigments (VAZ) per total chlorophyll amount, and (D) ratio of total chlorophylls to total carotenoids (Chl *a*+*b*/Car *x*+*c*) in needles within each examined level (whorl – W5, W8, W10, W15) of spruce crowns. Values presented show means ± standard deviation (vertical bars) of data measured during the cloudy day (left column) and sunny day (right column). Data followed by the same letter indicate a non-significant statistical difference ($P < 0.05$; Student's t-test) ($n = 20$).

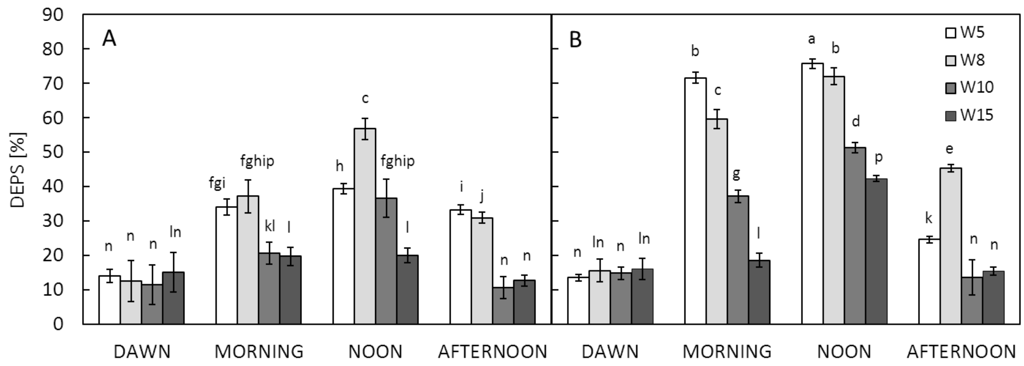

Fig. 3 Diurnal changes in de-epoxidation state of xanthophyll cycle pigments (DEPS) in needles from the 5th, 8th, 10th, and 15th whorl (W) on (A) the cloudy day and (B) the sunny day. Means (columns) and standard deviations (vertical bars) are presented (n = 5). Data followed by the same letter indicate statistically non-significant differences ($P > 0.05$; Student's t-test).

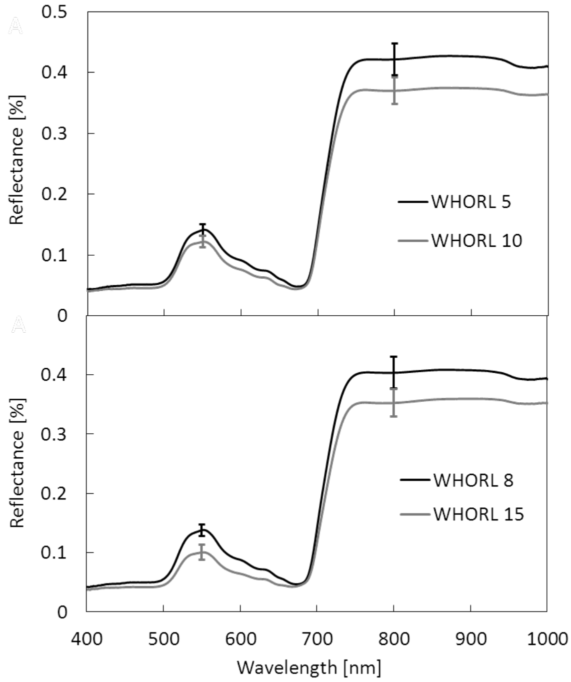

Fig. 4 Reflectance spectra of spruce needle samples measured during both experimental days within each crown level. The curve indicates the mean of 24 needle measurements performed for each whorl during both days; error bars indicate two-sided standard deviations in reflectance at 550 nm and 800 nm.

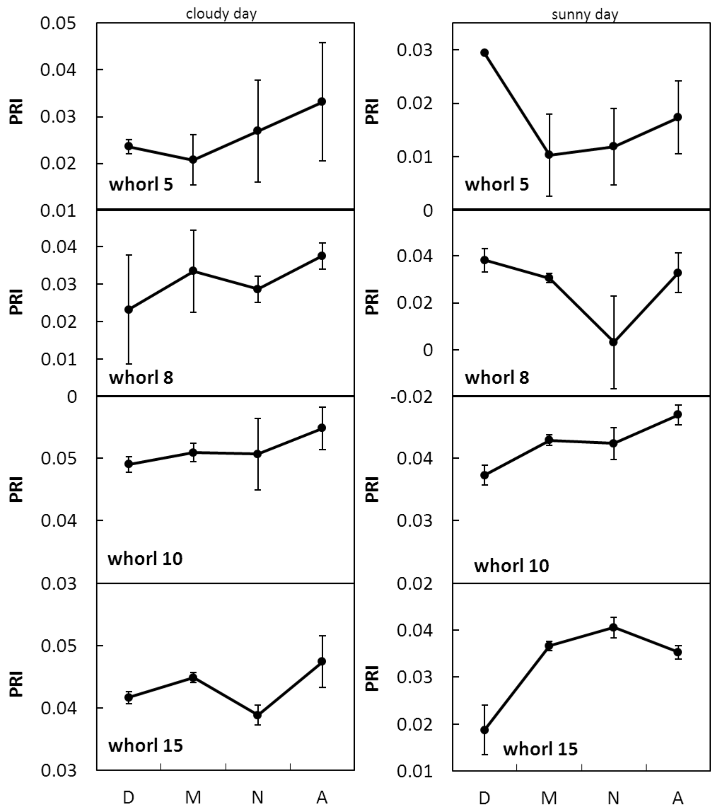

Fig. 5 Diurnal course of the PRI index calculated from needle reflectance measurements on needles from the 5th, 8th, 10th, and 15th whorl during the cloudy and sunny day. Each dot represents the mean of three measurements performed per whorl and time and vertical bars show ± standard deviation. Abbreviations: D ~ dawn, M ~ morning, N ~ noon, and A ~ afternoon.

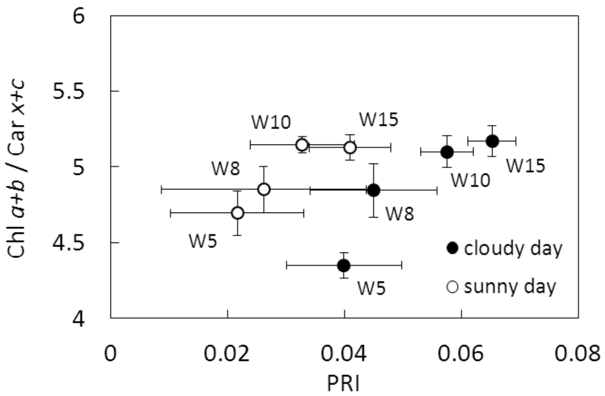

Fig. 6 Relationship between PRI values retrieved from 12 reflectance measurements of four investigated crown whorls (5th, 8th, 10th and 15th whorl from crown top) and Chl *a+b*/Car *x+c* ratios of these needles as averaged from 20 measurements conducted on the cloudy and sunny day. Error bars indicate the measurement standard deviation.

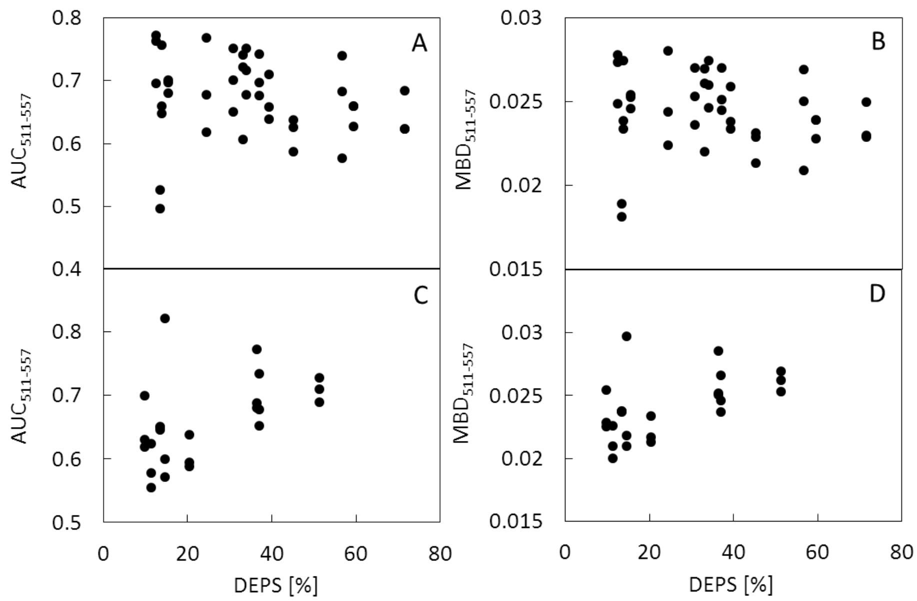

Fig. 7 Relationship between the de-epoxidation state of xanthophyll cycle pigments (DEPS) and Area Under Curve (AUC) and Maximal Band Depth (MBD) of continuum removed reflectance of the 5th and 8th whorl needles (A and B, n=42) and the 10th whorl needles (C and D, n=24) between 511-557 nm. Data of the 15th whorl are not shown for insufficient sensitivity of the $ANMB_{511\text{-}557}$ index to DEPS.

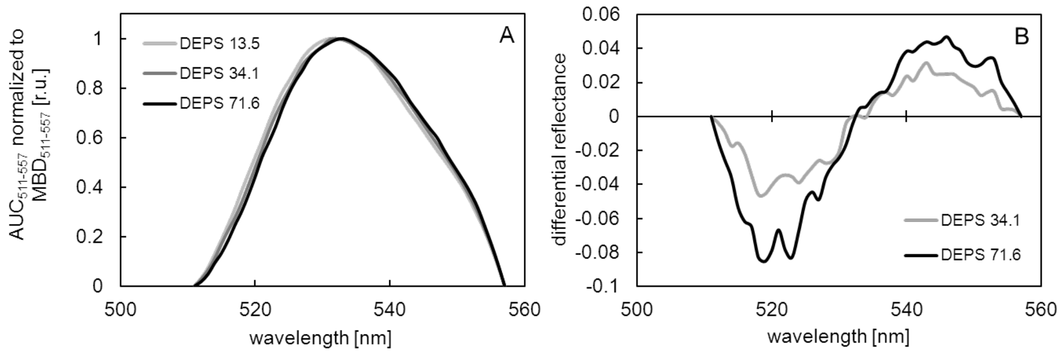

Fig. 8 (A) Area Under Curve (AUC) of continuum removed reflectance of Norway spruce needles between 511 – 557 nm normalized to Maximal Band Depth (MBD) of $AUC_{511\text{-}557}$. (B) Normalized area under continuum removed reflectance of two needle samples with de-epoxidation state of xanthophyll cycle pigments (DEPS) equal to 34.1% and 71.6%, respectively, subtracted from the needle sample with DEPS of 13.5%.

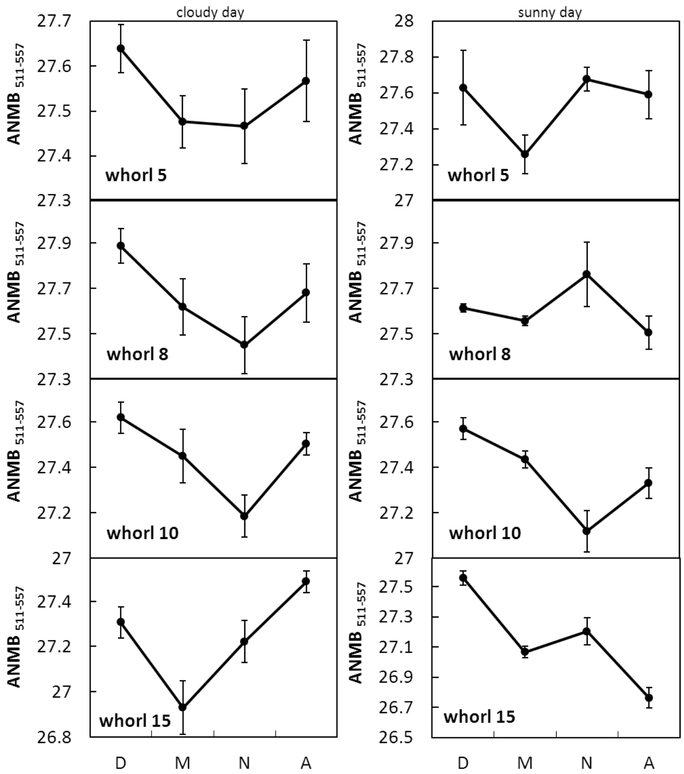

Fig. 9 Diurnal course of the $ANMB_{511\text{-}557}$ index calculated from the reflectance measured of needles from 5th, 8th, 10th, and 15th whorl during the cloudy and sunny day. Each dot represents the mean of three measurements performed per whorl and time. Vertical bars show ± standard deviation. Abbreviations: D ~ dawn, M ~ morning, N ~ noon, and A ~ afternoon.

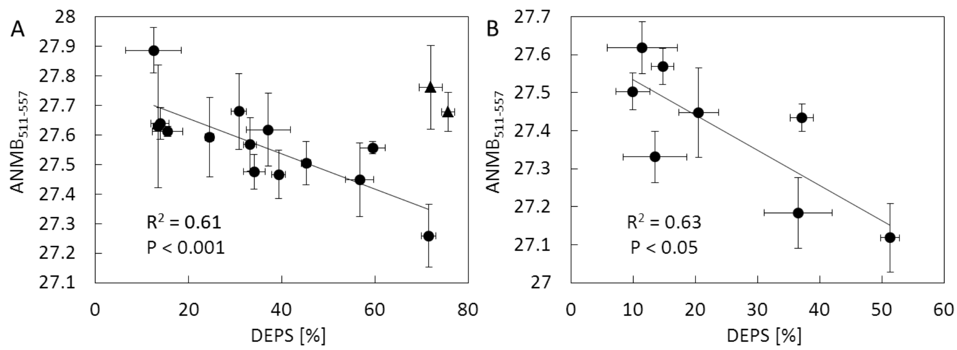

Fig. 10 Dependency between mean values of $ANMB_{511\text{-}557}$ and DEPS in (A) needles of the 5^{th} and 8^{th} whorl together (n = 14) (noon collections displayed as triangles were excluded from R^2 computation), and (B) needles of the 10^{th} whorl (n = 8). Average values ± standard deviation of the vegetation indices were calculated from 3 leaf reflectance signatures and average DEPS values ± standard deviation were calculated from 5 samples measured during the measurement cycle in the diurnal course.